

Study on the Use of Discretized Sliding-Mode Controller in DC-DC Switching Regulators

Somnath Maity *Member, IEEE*, Debjyoti Roy

Abstract—In this paper, we study the application of discretization of equivalent SM controller in DC-DC buck converters. Based on this control logic, we derive the two-dimensional (2-D) piecewise smooth (PWS) discontinuous map of the converter system. Some inherent dynamical properties of system's steady-state behaviors (i.e., the bifurcation behaviors) are also studied. The presented one- and two-parameter bifurcation digrams show the domains of existence of different oscillatory modes and their sequence of occurrence of the converter system, which are quite different from the bifurcation behaviors observed in 2-D PWS continuous maps [1].

Index Terms—Sliding mode (SM) control, digital sliding mode controller, DC-DC converter, 2-dimensional piecewise smooth (PWS) discontinuous map, complexity.

I. INTRODUCTION

The sliding mode (SM) controller is well known for its robustness and guaranteed stability under parameter variations and external perturbations [2], [3]. In spite of these unique advantages, it is practically impossible to implement the ideal SM controller for real-life variable structure power electronics systems. Ideally, the SM controller operates at infinite switching frequency, so that, the controlled variables can track the switching surface to achieve the desired dynamic response and steady state system operation [4]. This typical requirement results in excessive switching losses, inductor and transformer core losses, and electromagnetic interference (EMI) noise, and thereby, challenges the feasibility of applying SM controller in real-life applications.

One way to constrict this infinite switching frequency within a practical range is by incorporating the boundary layers around the sliding surface. Over the past decade, numerous control techniques, such as, bang bang control [5], [6], adoptive hysteresis control [7], [8], and fixed frequency control [9], [10] have been reported. In most of the cases, the SM controllers are implemented in analog domain, and the switching frequency has been restricted by using the concepts of hysteresis-modulation (HM) or delta-modulation technique. Once the SM controller is implemented for real systems, it is then transformed into a finite switching quasisliding-mode (QSM) controller. The proximity of QSM controller will be closer to the ideal one, if the switching frequency tends toward infinity.

However, the implementation of SM controllers in digital platforms also allows the fixed frequency switching operation. Because of the existence of a QSM band around the switching surface [11], [12], such controllers inherently work

like a boundary layered SM controller, and which can be used successfully to eliminate the chattering [12] across the switching manifold. However, since the trajectory after intersecting the switching manifold leaves this manifold, the invariance property enjoying in a continuous SM control may deteriorate drastically. Studies on this subject have been reported recently, where the investigations are normally based on two distinct approaches. One is the discrete-time sliding mode control approach [13], [14], and other is the direct discretization of equivalent SM control using Zero-Order-Hold (ZOH) circuit [15]. The use of ZOH circuits however show various kinds of irregularities including subharmonic oscillations, chaos, and coexisting attractor in a simple 2-dimensional (2-D) system [15], [16], [17]. In order to evaluate such quantitative discretization behaviors and to develop the preventive measures for these unwanted behaviors, it is therefore of practical importance to study the discretization effect of SM controllers.

In this paper, we apply the discretized equivalent SM controller in DC-DC converter and some inherent dynamical properties are studied. The system steady-state behaviors are discussed using the 2-D discontinuous maps. Lower bounds of sampling interval of the ZOH circuit is also obtained numerically.

II. EQUIVALENT CONTROL BASED SM CONTROLLED BUCK CONVERTER AND ITS DIGITAL REALIZATION

The SM controller provides an averaged control law [18] to necessarily maintain the state trajectory on the sliding manifold. However, the discretized models of the actual dynamical systems may have some properties different from the original one. For instance, for a differential equation having a periodic orbit, its discretized system does not necessarily have a corresponding periodic orbit. On the other hand, for a well-behaved continuous-time system with no periodic oscillations, may have periodic behaviors once it is discretized. Here, we discuss this with an example of power electronics converter.

A. SM Controlled Buck Converter in Continuous-time Domain

For a SM controlled converter under continuous conduction mode (CCM) of operation (see Fig. 1), the general control variables can be defined as

$$\begin{aligned} x_1 &= V_{\text{ref}} - v \\ x_2 &= \frac{dx_1}{dt} = -\frac{dv}{dt} = -\frac{i}{C} + \frac{v}{RC} \end{aligned} \quad (1)$$

where C is the capacitance, L is the inductance, R is the load resistance, i is the inductor current, and v is the capacitor

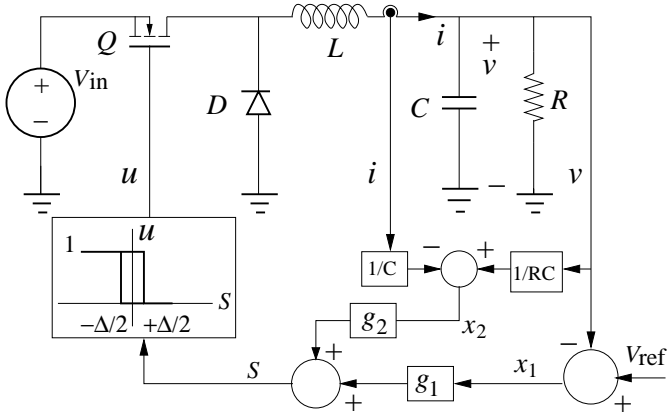


Fig. 1. Sliding mode controlled buck converter.

voltage. Substitution of the behavioral model of buck converter into (1) gives the system dynamical equation as

$$\begin{aligned} \frac{dx_1}{dt} &= x_2 \\ \frac{dx_2}{dt} &= -\frac{1}{LC}x_1 - \frac{1}{RC}x_2 + \frac{V_{ref}}{LC} - \frac{V_{in}}{LC}u. \end{aligned} \quad (2)$$

In state-space model, it can also be expressed as

$$\frac{dx}{dt} = Ax + Bu + D \quad (3)$$

where

$$A = \begin{pmatrix} 0 & 1 \\ -1/LC & -1/RC \end{pmatrix}, B = \begin{pmatrix} 0 \\ -V_{in}/LC \end{pmatrix},$$

$$D = \begin{pmatrix} 0 \\ V_{ref}/LC \end{pmatrix}, x = \begin{pmatrix} x_1 \\ x_2 \end{pmatrix},$$

and V_{in} is the input voltage with discontinuous control input

$$u = \begin{cases} 1 & \text{if } S < -\Delta/2 \\ u_{eq} & \text{if } -\Delta/2 < S < +\Delta/2 \\ 0 & \text{if } S > +\Delta/2 \end{cases} \quad (4)$$

to drive the power switch Q . The objective of this control logic is that regardless of the starting position $x(0)$, the controller will perform a control decision that will drive the system trajectory on either side of the switching surface

$$S = g_1x_1 + g_2x_2 = Gx = 0 \quad (5)$$

where $G = [g_1 \ g_2]$, to converge to it, for all $t > 0$. The trajectory is then said to be in sliding mode if the motion within a small vicinity around the surface $\{S: -\Delta/2 < S < +\Delta/2\}$ is maintained, and consequently directed toward the equilibrium point. In other words, it can be said that the SM controller is performing its control decision by utilizing the sliding plane as a reference path, on which the trajectory will track and eventually converge to the origin to achieve desired steady-state operation satisfying the inequality conditions

$$\lim_{S \rightarrow 0^+} \frac{dS}{dt} < 0 \text{ and } \lim_{S \rightarrow 0^-} \frac{dS}{dt} > 0 \quad (6)$$

when $\Delta \rightarrow 0$. Here, the conditions (6) are called the sliding mode *reachability conditions* or *existence conditions* [4], [18].

For an ideal SM controlled buck converter, these conditions can be easily derived from (5) and (6), as

- 1) If $S \rightarrow 0^+$, $dS/dt < 0$; $u = 1$, then

$$\frac{dS}{dt} = \frac{-g_2x_1}{LC} + \left(g_1 - \frac{g_2}{RC}\right)x_2 - g_2 \left[\frac{V_{in}}{LC} - \frac{V_{ref}}{LC}\right] < 0$$

- 2) If $S \rightarrow 0^-$, $dS/dt > 0$; $u = 0$, then

$$\frac{dS}{dt} = \frac{-g_2x_1}{LC} + \left(g_1 - \frac{g_2}{RC}\right)x_2 + \frac{g_2V_{ref}}{LC} > 0.$$

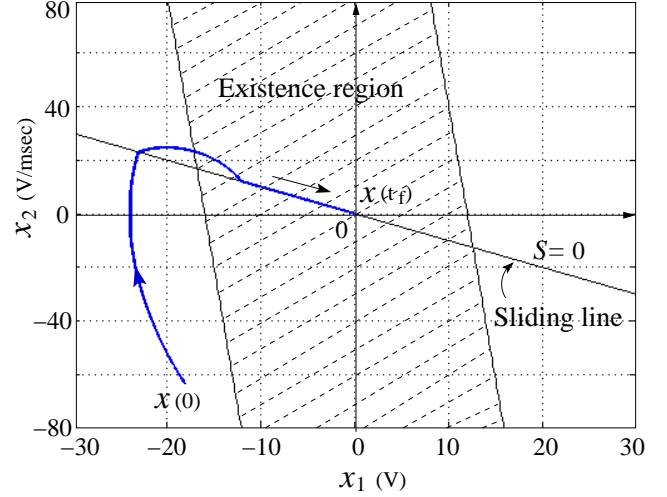


Fig. 2. Trajectory of SM controlled buck converter showing the switching and sliding motion. The parameter values are $L = 2.5\text{mH}$, $C = 32\mu\text{F}$, $R = 15\Omega$, $V_{in} = 28\text{V}$, $V_{ref} = 12\text{V}$, $g_1 = 10$, $g_2 = 0.005$, and $\Delta = 0.2$.

In other word, one can express these reachability conditions or the regions of existence as

$$0 < -\frac{g_2}{LC}x_1 + \left(g_1 - \frac{g_2}{RC}\right)x_2 + \frac{g_2V_{ref}}{LC} < \frac{g_2V_{in}}{LC}. \quad (7)$$

Once the trajectory reaches S and reachability conditions (7) hold, the ideal sliding motion starts, and the trajectory following the reduced order dynamics

$$\frac{dx_2}{dt} - (g_1/g_2)x_2 = 0 \quad (8)$$

will be asymptotically stable. The system will be globally stable for any initial position $x(0)$, if there exists $t_s > 0$. However, if the reachability condition does not hold, it can be shown that after successive finite number of switchings the reachability condition must be satisfied [4].

In Fig. 2, an example trajectory of SM controlled buck converter is shown, where without satisfying the existence condition, the trajectory starting from an initial point $x(0) = (-18, -6.3830 \times 10^4)$ is intersecting by the switching manifold $S = 0$ at time $t = t_s$ (where $t_s > 0$). Once the existence condition is satisfied just after first intersection, a sliding motion starts and trajectory approaches to the equilibrium point $x(t_f) \approx 0$ along the sliding line with a very high switching frequency as shown in Fig. 3. The frequency of switching operation are normally fixed, and controlled by varying the width of the hysteresis band Δ . However, this way of switching frequency fixation makes the state function

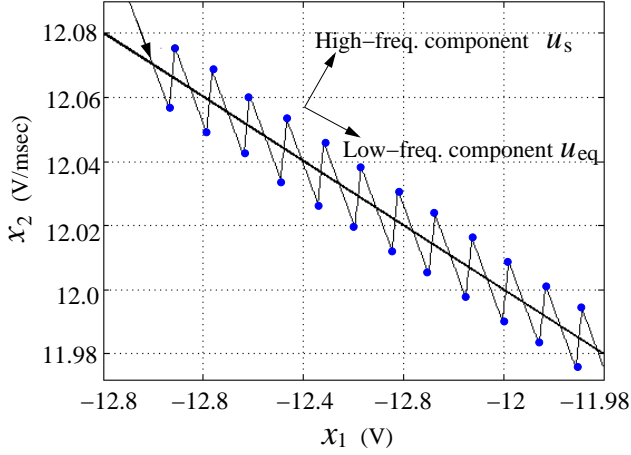


Fig. 3. Trajectory showing the high and low frequency components along the sliding surface. Dots indicate the switching instants on the boundary layers. All parameter values are same as in Fig. 2.

discontinuous across $S = G^T x = 0$, therefore, violates the existence and uniqueness of the solution of system (3). Fillipov's method and Utkin's equivalent control concept have been successfully used to overcome this problem. The main concept behind such methods [2] is that in the vicinity of the sliding surface, motion velocity vector is always tangential to the sliding surface, and the resulting dynamics

$$\frac{dx}{dt} = Ax + Bu_{eq} + D \quad (9)$$

is only governed by a smooth control law $u = u_{eq}$ without any discontinuity. Unfortunately, it only serves as a mathematical description of such motion, but impossible to implement in real-life applications. A lot of control algorithms employ equivalent control as a component of the real control, which is usually defined as a composition of two isolated components $u = u_{eq} + u_s$ as shown in Fig. 3.

Although, the motion of trajectory is defined by the composition of two components $u \in (u_{eq}, u_s)$ with different time-scale, the slow-moving (low-frequency) component u_{eq} is responsible for the continuous trajectory that follows the desired reduced order dynamic behavior after the sliding mode starts, and which can be easily derived from (8) and (9), satisfying $dx/dt = 0$ as

$$u_{eq} = -(GB)^{-1} [GAx + GD] \quad (10)$$

where $(GB)^{-1} \neq 0$. Substituting u_{eq} into (9) yields the slow-scaled dynamical equation

$$\frac{dx}{dt} = (A - B(GB)^{-1}GA)x - B(GB)^{-1}GD + D = 0$$

whose roots determine the asymptotic stability of the system. If the roots are in left-half of s -plane, then the system is stable. Whereas the high frequency component u_s forces the trajectory to move alternatively between $+ve$ and $-ve$ direction of $S = 0$ in such a way that just after every switching events, trajectory always points towards the switching manifold, governed by discontinuous switching law

$$u_s = -\frac{1}{2}(GB)^{-1} (1 + \text{sgn}(S)) \quad \text{where } \text{sgn}(S) = \begin{cases} 0 & \text{if } S < 0 \\ 1 & \text{if } S > 0 \end{cases}$$

B. Discretization of SM Control

Let us now investigate the effect of discretization of equivalent SM controller in buck converter. In Fig. 4, the switching signal u is generated by comparing switching function S sampled over the time interval T with a zero reference value. This can be implemented by using a comparator used as a zero crossing detector followed by a Sample-and-Hold (S/H) circuit. The S/H circuit is one of the main functional block in all digital signal processors causing the time delay in control circuit. Due to this internal time delay, the control signal $u_n = u_{eq,n} + u_{s,n}$ at the moment $t_n = nT$ will be constant for the time interval (t_n, t_{n+1}) , where $t_{n+1} = (n+1)T$ and T is the sampling interval. Based on (10) and (11), we can write these as

$$u_{eq,n} = -(GB)^{-1}(GAx_n + GD) \quad (11)$$

$$u_{s,n} = -\frac{1}{2}(GB)^{-1}(1 + \text{sgn}(S_n)). \quad (12)$$

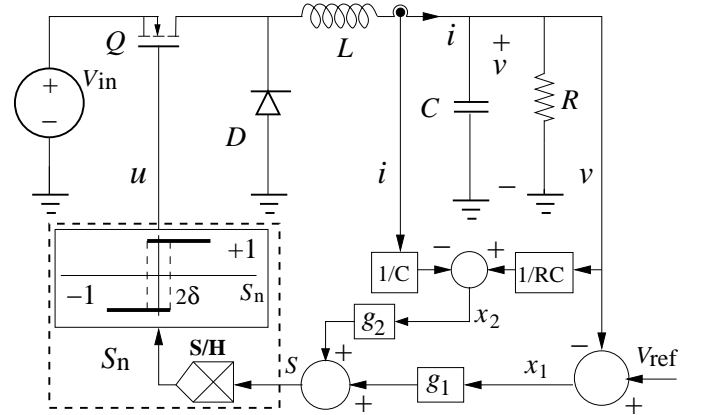


Fig. 4. Schematic of discretized SM controlled buck converter

Moreover, during the time T , the inter-sample motion will deviate from sliding hypersurface $S_n = 0$, and chatter within a specific band is called the QSM band (see Fig. 4), defined by

$$\{-\delta \leq S_n(x_n, T) \leq +\delta\} \quad (13)$$

where δ is a function of x_n and T . When $\delta \rightarrow 0$, the QSM controller becomes an ideal SM controller. Theoretically it is only possible when sampling interval time $T \rightarrow 0$. For the practical parameter values $L=2.5$ mH, $C=32$ μ F, $R=15$ Ω , $V_{in}=26$ V, $V_{ref}=12$ V, $g_1=1$, $g_2=0.001$, and $T=10$ μ sec, the converter is globally stable for $t > 0$ as shown in Fig. 5. Once the trajectory enters into the existence regions, the quasi-sliding motion starts and moves toward the quasi-equilibrium point. Therefore, from equivalent SM control law, one could expect that the system will be asymptotically stable, if the eigenvalues of the closed system, given by

$$x_{n+1} = e^{AT} x_n + \int_0^T e^{A\tau} (Bu_n + D) d\tau \quad (14)$$

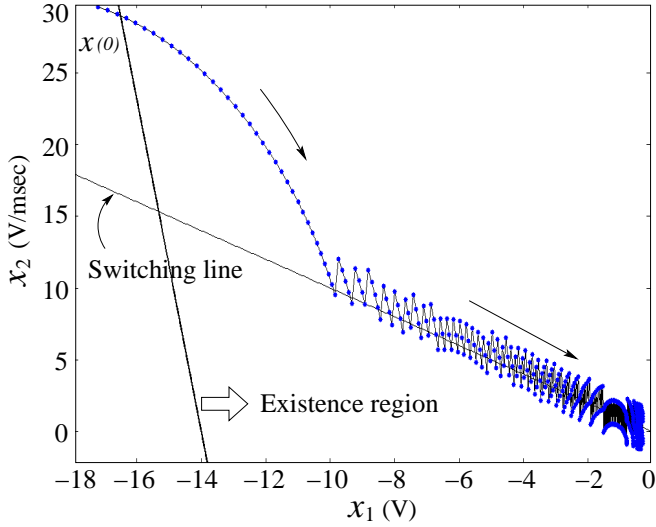


Fig. 5. Trajectory evolution of discretized SM controlled buck converter with sampling time interval $T=10\mu\text{sec}$. The other parameters value are : $L = 2.5\text{mH}$, $C = 32\mu\text{F}$, $R = 15\Omega$, $V_{\text{in}} = 26\text{V}$, $V_{\text{ref}} = 12\text{V}$, $g_1 = 1$, and $g_2 = 0.001$. Dots indicate the sampled value of switching function S over time interval T .

or,

$$x_{n+1} = \left[e^{AT} - B(GB)^{-1}GA \int_0^T e^{A\tau} d\tau \right] x_n + (I - B(GB)^{-1}G) \int_0^T e^{A\tau} D d\tau \quad (15)$$

are within the unit circle where $u_n = u_{eq,n}$.

However, due to fast-moving control component $u_{s,n}$ the system will not be asymptotically stable, i.e., the states do not converge to zero in finite time. It will force the trajectory to jitter alternatively between two halves of the switching plane $S_n = 0$, and makes the system oscillatory. The dynamics around the switching surface can be then derived by substituting (12) into (14), and equating slowly moving component to zero, as

$$x_{n+1} = e^{AT}x_n + \int_0^T e^{A\tau} D d\tau - \frac{1}{2}(GB)^{-1}(1 + \text{sgn}(S_n)) \int_0^T e^{A\tau} B d\tau.$$

In compact form, it can also be written as

$$x_{n+1} = \begin{cases} \Phi x_n + \Gamma & \text{if } S_n < 0 \\ \Phi x_n + \Gamma - \Pi & \text{if } S_n > 0 \end{cases} \quad (16)$$

where

$$\Phi = e^{AT}, \quad \Gamma = \int_0^T e^{A\tau} D d\tau, \\ \Pi = (GB)^{-1} \int_0^T e^{A\tau} B d\tau \quad \text{and} \quad S_n = Gx_n.$$

The equation (16) represents a hybrid dynamical system switching between two discrete-time invariant linear systems with two different equilibrium points. For autonomous part of the systems, eventually the trajectory will be attracted

by the fixed points $x_n^* = (I - \Phi)^{-1}(\Gamma + \Pi)$ and $x_n^* = (I - \Phi)^{-1}(\Gamma - \Pi)$ respectively. However, with switching involved in the system the dynamical behavior becomes much more complex. As an example, the discretized switching function dynamics S_n of the SM controlled buck converter is shown in Fig. 6. As the system state x_n evolves, the function $\text{sgn}(S_n)$ forms a sequence of binary value -1 and +1. After the initial transient, once the system trajectory is eventually attracted by the trapped region in finite time, it stays within a bounded region followed by a fast-scale periodic orbit with different periodicities. Fig. 7 shows the typical examples of period-2, period-5, and aperiodic trajectory in discrete-time domain at different input voltages 24.5V, 31.5V, and 28.1V respectively. The occurrence and existence of such

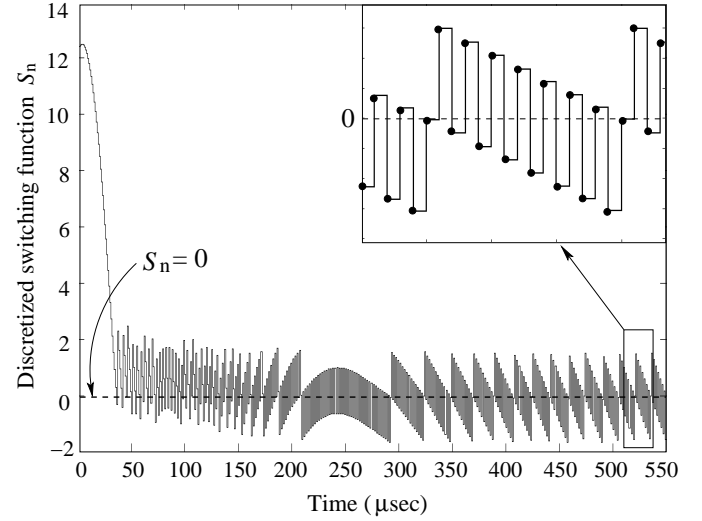


Fig. 6. A representative discretized switching function dynamics showing the period-16 orbit in steady state condition. The parameters value are same as in Fig. 5.

kind of complex behaviors are quite different from the behaviors observed in two-dimensional (2-D) piecewise smooth (PWS) continuous maps, which can be however successfully explained by recently developed bifurcation theory for 2-D PWS discontinuous maps [19].

III. COMPLEX BEHAVIORS OF DISCRETIZED SM CONTROLLED BUCK CONVERTER

Let us now examine the effect of this discontinuity on the system's bifurcation behavior. In order to understand the bifurcation of (16), one has to obtain eigenvalues of the fixed points at the two sides of the borderline, and from that, the value of trace and the determinant. Here, the explanations of the observed bifurcation have to be obtained by analysing the PWS discontinuous maps of (16) in the neighborhood of the borderline

$$x_{n+1} = \begin{cases} J_L x_n + \Gamma + \Pi, & \text{if } S_n < 0 \\ J_R x_n + \Gamma - \Pi, & \text{otherwise} \end{cases} \quad (17)$$

where

$$J_L = \left. \frac{\partial(\Phi x_n + \Gamma + \Pi)}{\partial x} \right|_{x^*} = \Phi, \quad J_R = \left. \frac{\partial(\Phi x_n + \Gamma - \Pi)}{\partial x} \right|_{x^*} = \Phi$$

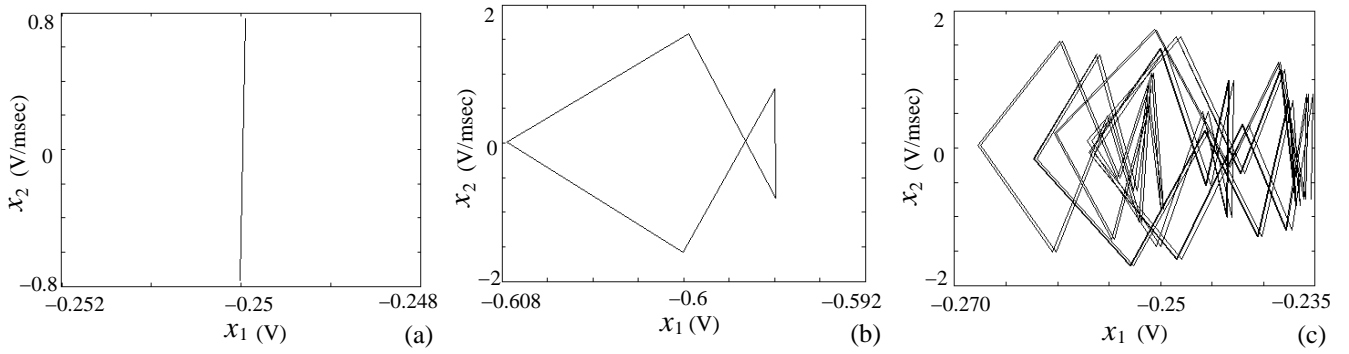


Fig. 7. Examples of: (a) period-2, (b) period-5, and (c) aperiodic trajectory in discrete domain. The corresponding input voltages V_{in} are 24.5V, 31.5V, and 18.1V respectively.

are the Jacobian matrix of the system at a fixed point in $L = \{x_n^* \in \mathbb{R}^2 : S_n < 0\}$ and in $R = \{x_n^* \in \mathbb{R}^2 : S_n > 0\}$ respectively. The normal form (17) follows from that derived for PWS continuous maps, with discontinuity 2Π . The fixed point of the system (17) on both the side of the boundary $S_n = 0$ are $x_L^* = (I - \Phi)^{-1}(\Gamma + \Pi)$ and $x_R^* = (I - \Phi)^{-1}(\Gamma - \Pi)$. If $x_L^* = \{S_L^* < 0\}$ condition holds, the fixed point exists. Else it does not. However, for $x_L^* = \{S_L^* < 0\}$, iteration from initial conditions in left half are influenced by the nonexistent fixed point, which is called virtual fixed point, and denoted by \bar{x}_L^* . Similarly, when the condition $x_R^* = \{S_R^* > 0\}$ is fulfilled, the fixed point exist; else it is virtual fixed point denoted by \bar{x}_R^* . In this case, both sides fixed points $\bar{x}_L^* = (12.0 \ 0)^T$ and $\bar{x}_R^* = (-12.0 \ 0)^T$ are virtual attractors. Thus, any initial state in the L is drawn towards the virtual attractor \bar{x}_L^* situated in R . However as soon as it cross the borderline $S_n = 0$, it is drawn back toward the virtual attractor \bar{x}_R^* situated in L . The state therefore locked between the two virtual fixed attractors and that results a bounded orbit coexisting with multiple attractors. The same behavior is exhibited by an initial state in R . This closed orbit will be then high periodic or chaotic orbits.

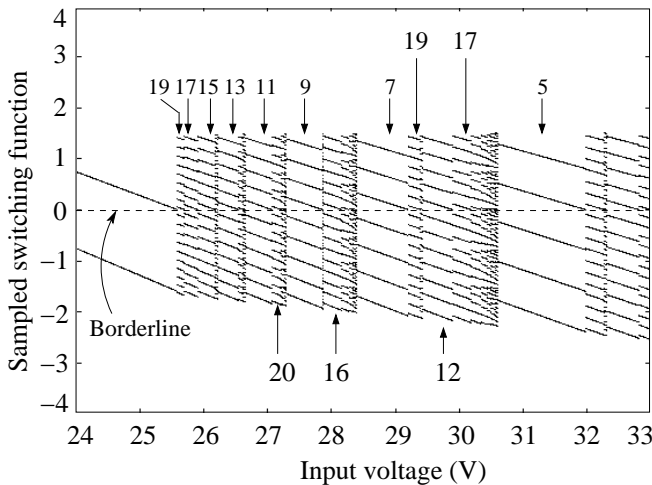


Fig. 8. Bifurcation diagram of discretized SM controlled buck converter showing the periodic orbit with different periodicities when V_{in} is varied from 24 to 33V. The other parameters are: $L = 2.5mH$, $C = 32\mu F$, $R = 15\Omega$, $V_{ref} = 12V$, $g_1 = 1$, $g_2 = 0.001$, $T = 10\mu sec$.

Among these closed orbits, the condition of the existence

of the period-1 and period-2 fixed point was reported earlier in [20]. In this paper, we apply those concepts to facilitate the understanding of the complex dynamics of discretized SM controlled buck converter. Since there exists no period-1 attractor in this system, here, we will consider the existence of period-2 attractor only. It is possible to show the conditions of the existence of period-2 fixed points of 2-D maps. The detail analysis is not shown here. However, since the system is linear in each side of the border, period-2 (or higher) fixed points can not exist with all points in L or all points in R . In some regions of parameter space, a period-2 fixed point may exist with one point in L and one point in R .

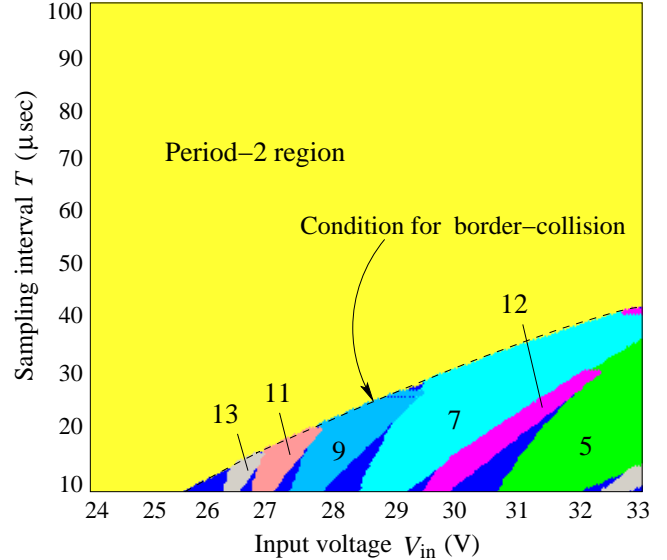


Fig. 9. The domains of existence of different oscillatory modes in $V_{in} - T$ parameter space: $\{24 < V_{in} < 33; 10 < T < 100\}$. The parameter values are taken same as in Fig. 8. Here, numbers indicate the domains of existence of those periodic orbits and the unmarked domains represents the regions of aperiodic behavior or periodicities higher than 13.

Here, we observe that the set of bifurcation curves of these maps give a structure, which are different from the PWS continuous maps. As an example, a representative bifurcation diagram is shown in Fig. 8. It has been seen that the equivalent SM controlled buck converter exhibits stable period-2 operation when it operates at input voltage less than 25.59V. If

the input voltage V_{in} increases further through $V_{in} = 25.59V$, the period-2 orbit vanishes through border-collision bifurcation and a high periodic orbit, for example, period-19 having symbolic sequence $LRL\dots$ with period increment and Faray tree sequence comes into existence. With further increment of V_{in} , the symbolic sequence gets reversed, i.e., the symbol sequence $RLR\dots$ comes into existence.

This property can be easily conjectured even by a quick numerical computation and graphical representation of the regions of existence of stable cycles of different periods. In fact, for any value of the discontinuity, the numerically computed 2-D bifurcation diagram in the parameter plane $[V_{in}, T]$ has a certain structure (see Fig. 9), where each colored region corresponds to a cycle of fixed period according to the numbers reported in the picture. Such regions are usually called periodicity regions (or periodicity tongues due to their shape [21]). Moreover, for parameters belonging to the boundary of a periodicity region a border-collision occurs involving the cycles existing inside the region.

IV. CONCLUSION

To restrict the switching frequency within a practical range, the realization of Utkin's equivalent control law is normally achieved by using boundary layers controller or QSM controller. In this paper, we have shown that the SM controller implemented in the digital platform are inherently a QSM controller, therefore, amenable to the same treatment. We have also investigated the discretization effects of SM controller in the DC-DC buck converters. It is seen that, the dynamics under this control schemes can be successfully modeled by the 2-D discontinuous maps reported earlier. Based on the numerical simulations, we have also shown the domain of existence of different periodic orbits and their occurrence into $V_{in} - T$ parameter space, which are quite different from bifurcation behaviors obtained from 2-D PWS continuous maps. The deeper understanding of such behaviors and their physical importance in real-life applications however will be discussed in future.

REFERENCES

- [1] S. Maity, D. Tripathy, T. K. Bhattacharya, and S. Banerjee, "Bifurcation analysis of PWM-1 voltage-mode controlled buck converter using the exact discrete model," *IEEE Transactions on Circuits and Systems-I*, vol. 54, no. 5, pp. 1120–1130, May 2007.
- [2] V. Utkin, J. Guldner, and J. X. Shi, *Sliding Mode Control in Electromechanical Systems*. London, U.K: Taylor & Francis, 1999.
- [3] W. Gao and J. C. Hung, "Variable structure control of nonlinear systems: A new approach," *IEEE Transactions on Industrial Electronics*, vol. 40, no. 1, pp. 45–55, February 1993.
- [4] C. Edwards and S. K. Spurgeon, *Sliding Mode Control: Theory and Applications*. London, U.K: Taylor & Francis, 1998.
- [5] M. Carpita and M. Marchesoni, "Experimental study of a power conditioning system using sliding mode control," *IEEE Transactions on Power Electronics*, vol. 11, no. 5, pp. 731–742, September 1996.
- [6] V. M. Nguyen and C. Q. Lee, "Indirect implementations of sliding-mode control law in buck-type converters," *Applied Power Electronics Conf. and expo.(APEC)*, vol. 1, pp. 111–115, March 1996.
- [7] H. Sira-Ramirez, "Sliding mode δ -modulation control of a buck converter," in *Proc.42nd IEEE Conference on Decision and Control*, vol. 3, pp. 2999–3004, December 2003.
- [8] S. C. Tan, Y. M. Lai, C. K. Tse, and M. K. H. Cheung, "Adaptive feed-forward and feedback control schemes for sliding mode controlled power converters," *IEEE Transactions on Power Electronics*, vol. 21, no. 1, pp. 182–192, January 2006.

- [9] S. K. Mazumder and S. L. Kamisetty, "Experimental validation of a novel multiphase nonlinear vrm controller," *IEEE Power electronics specialists conferenc*, vol. 3, pp. 2114–2120, 2004.
- [10] S. C. Tan, Y. M. Lai, C. K. Tse, and M. K. H. Cheung, "A fixed frequency pulsewidth modulation based quasi-sliding-mode controller for buck converters," *IEEE Transactions on Power Electronics*, vol. 20, no. 6, pp. 1379–1392, November 2005.
- [11] K. Furuta, "Sliding mode control of a discrete system," *Systems & Control Letters*, vol. 14, no. 2, pp. 145–152, February 1990.
- [12] W. Gao, Y. Wang, and A. Homaifa, "Discrete-time variable structure control systems," *IEEE Transactions on Industrial Electronics*, vol. 42, no. 2, pp. 117–122, April 1995.
- [13] C. Milosavljevic, "Discrete-time VSS" in *Variable structure System: From Theory to Applications*. London, U.K: IEE Press, 2004, vol. 66.
- [14] A. Jafari Koshkouei and A. S. I. Zinober, "Sliding mode control of discrete-time systems," *Journal of Dynamic Systems, Measurement, and Control*, vol. 122, no. 4, pp. 793–802, December 2000.
- [15] Z. Galias and X. Yu, "Analysis of zero-order holder discretization of two-dimensional sliding-mode control systems," *IEEE Transactions on Circuits and Systems-II*, vol. 55, no. 12, pp. 1269–1273, December 2008.
- [16] X. Yu, B. Wang, Z. Galias, and G. Chen, "Discretization effect on equivalent control based multi-input sliding mode control systems," *IEEE Transactions on Automatic Control*, vol. 53, no. 6, pp. 1563–1569, July 2008.
- [17] B. Wang, X. Yu, and G. Chen, "ZOH discretization effect on single-input sliding mode control systems with matched uncertainties," *Automatica*, vol. 45, no. 1, pp. 118–125, January 2009.
- [18] V. I. Utkin, "Variable structure systems with sliding modes," *IEEE Transactions on Automatic Control*, vol. 22, no. 2, pp. 212–222, 1977.
- [19] B. Rakshit, M. Apratim, P. Jain, and S. Banerjee, "Bifurcation phenomena in two-dimensional piecewise smooth discontinuous maps," *Chaos-Interdisciplinary Journal of Nonlinear Science*, vol. 20, no. 3, pp. 3 422 475–3 422 487, 2010.
- [20] P.S. Dutta, B. Routroy, S. Banerjee, and S. S. Alam, "On the existence of low-period orbits in n -dimensional piecewise linear discontinuous maps," *Nonlinear Dynamics*, vol. 53, no. 4, pp. 369–380, December 2008.
- [21] I. Sushko, L. Gardini, and T. Puu, "Tongues of periodicity in a family of two-dimensional discontinuous maps of real mobilus type," *Chaos, Solitons and Fractals*, vol. 21, no. 2, pp. 403–412, 2004.